

TURBULENT-REYNOLDS-NUMBER AND TURBULENT-FLAME-QUENCHING INFLUENCES ON EXPLOSION SEVERITY WITH IMPLICATIONS FOR EXPLOSION SCALING

C.L. Gardner, H. Phylaktou and G.E. Andrews

Department of Fuel and Energy, University of Leeds, Leeds LS2 9JT

Explosion severity is dependent on the turbulent burning rate which is related to the integral-length-scale of turbulence which in turn is a function of the characteristic obstacle scale. Methane/air explosions propagating with an approach flame speed of about 50 m/s, were made to interact with a turbulence-inducing obstacle in the shape of a bar-grid. The scale of these flat-bar grid obstacles was varied by changing the number of bars for fixed blockage ratios. The obstacle scale was taken as the bar width perpendicular to the flow direction of the propagating flame front.

In effect, the turbulent Reynolds number, R_t , was systematically changed from 2,500 to 215,000, by varying both the scale and intensity of turbulence. The maximum overpressure, rate of pressure rise and flame speed increased with an increase of R_t . The Karlovitz flame stretch factor, Ka , was also found to influence the explosion severity. The overpressures and the estimated turbulent burning velocity S_T , were shown to correlate well with R_t and also shown to separate into two distinct correlations identified by $Ka < 1$ or $Ka > 1$. There was evidence that Ka may be acting as a switch between full-burning and partial/local flame quenching (with associated lower overpressures) at a critical narrow range of Ka around unity. The results show that both the Ka number and the correct dependence on scale are important in providing the fundamental understanding framework for improving explosion scaling approaches used in industry today.

Keywords: Explosion, scaling, turbulent Reynolds number, flame quenching

INTRODUCTION

Current explosion scaling methods [1,2,3] are deduced from considerations of fundamental turbulent combustion models. Such models at present are derived from small scale experiments, at low turbulent Reynolds number (R_ℓ) with little or no variation of length-scale. Catlin & Johnson [2] estimated that in large scale vapour-cloud explosion tests with pipe arrays as obstacles [4,5], turbulent Reynolds numbers of the order of 70000 were induced, while it is estimated that atmospheric explosions can be associated with R_ℓ values in the range of 10^6 to 10^7 [6]. Most experimental flame structure studies and modelling of turbulent combustion have been carried out for regimes with R_ℓ generally below 20000, with the variation of R_ℓ achieved by changing the intensity of turbulence (u') rather than the length-scale (ℓ).

In this investigation, R_t was varied from 4,000 to 215,000 by systematic variation of both ℓ and u' . The influence of these parameters on explosion overpressures, rates of pressure rise and flame speeds, as well as on the derived turbulent burning velocities was investigated.

EXPERIMENTAL

Fifty 10% methane/air explosion tests at 16 different initial conditions were carried out in a 162 mm diameter cylindrical vessel with an L/D (length-to-diameter ratio) of 26. The vessel was mounted horizontally and closed at one end with its open end connected to a large dump vessel (2.5 m diameter) with a volume of 40 m³, more than 450 times greater than that of the test vessel. This arrangement allowed the simulation of open-to-atmosphere explosions with accurate control of both the test and dump vessel pre-ignition conditions.

A pneumatically actuated gate valve isolated the test vessel prior to mixture preparation. A vacuum pump was used to evacuate the test vessel before a 1 atm, 10% methane/air mixture was formed by partial pressures. The dump vessel was filled with air to a pressure of 1 atm. After mixture circulation, the gate valve was opened and spark ignition was effected at the centre of the test vessel ignition-end flange.

The obstacles were 3 mm thick mild steel single and multi-bar grid plates positioned at 6.2D from the spark. The obstacle characteristics are presented in Table 1. The characteristic obstacle-scale, b is defined as the individual bar width. For any single obstacle configuration each bar had the same width. The obstacles were designed so that the aerodynamic flow areas between the bars were also the same.

An array of thermocouples along the axial centreline of the test vessel was used to record the time of flame arrival. Pressure-time histories were recorded using Keller pressure transducers mounted at the ignition-end flange, halfway along (5D downstream of the obstacle) and at the end (17D from the obstacle) of the test vessel. Two others were located in the dump vessel. Pressure drop and pressure loss measurements were made using differential pressure transducers across the obstacle and this enabled the calculation of the velocity of the explosion-induced gas flow (U) through the obstacle, ahead of the propagating flame. Each test was repeated at least twice.

RESULTS

General effects of obstacles / influence of scale

Figure 1(a) shows the pressure traces recorded at the closed end of the test vessel for tests with a grid-bar obstacle of 30% BR with 1, 3 and 5 bars. The corresponding records of flame position against time are shown in Fig. 1(b). The general phenomena and mechanism associated with explosion development in tubular geometries with and without obstacles have been discussed elsewhere [7].

The turbulence of the fast unburnt gas flow downstream of the obstacle, induced by an initial fast elongated flame propagation, resulted in flame acceleration due to turbulent combustion. This gave rise to a rapid rate of pressure rise (dP/dt). As the flame propagated into the region of turbulence decay the pressure started to fall resulting in the pressure peak P_{max} . No rise in pressure recorded in the dump vessel prior to the flame exit from the test vessel indicated that the large dump vessel did not influence the explosion development inside the test vessel.

Figure 1(b) indicates maximum flame speeds upstream of the obstacle of the order of 50 m/s for all three obstacles (these flame speeds were similar in all tests). Downstream of the obstacle the average flame speed (approximated by the slope of the dotted fitted lines as 181, 207 and 247 m/s) increased with obstacle scale. This was in accord with the trends in both the rate of pressure rise and the maximum pressure attained.

The thermocouple time-of-flame-arrival data downstream of the obstacle, shown in Fig. 1(b) indicates the flame sometimes arrived at different positions almost simultaneously, while at other times it is shown to arrive at downstream positions before it arrived at neighbouring upstream ones. The high maximum flame speeds in this series of tests (150 to 650 m/s) and the associated high flame acceleration, may have limited the accuracy of the thermocouple technique. However, it will be shown later that most of the present explosions took place in what is described by researchers as the distributed reaction zone or the fragmented-flame regime with possible extinction areas. Therefore, the apparent time-of-arrival anomaly could simply be interpreted as further evidence of fragmented flame zones.

On a practical level this made it difficult to obtain sufficiently resolved and reliable flame speed data from first analysis of the thermocouple records. A simple smoothing procedure was applied to the recorded flame-arrival times so that local minima and maxima points on the derived flame speeds, inconsistent with neighbouring trends, were smoothed out. An example of such a flame speed record, which corresponds to the single-bar test in Fig. 1, is shown in Fig. 2.

In vapour cloud explosions it is usual to assume that the overpressure is proportional to the square of the flame speed [1,8]. A more detailed expression was given by Harrison and Eyre [5], based on the simplified acoustic theory given by Taylor [9], in terms of the flame speed Mach number. If the ambient pressure is atmospheric then the overpressure is given by:

$$P = \frac{2\gamma M^2}{1+M} \quad (\text{baro}) \quad (1)$$

Using a speed of sound of 340 m/s, $\gamma = 1.4$ and applying the averaged flame speeds downstream of the obstacle determined as in Fig. 1(b), i.e. 181, 207 and 247 m/s for the 5, 3 and 1 bar obstacle respectively, Eq. 1 returned overpressure values of 0.52, 0.65 and 0.86 baro. These compare well with the average overpressure after the obstacle shown in Fig. 1(a) for each of the tests.

The implication of this good agreement is that the mechanism of pressure generation in the present tests might be the same as that of vapour-cloud explosions, i.e. the pressure rise is due mainly to the inertia of the gas immediately ahead of the flame, and it is not significantly influenced by the confinement offered by the present geometry.

The pressure signal from the transducer at the test vessel exit showed that in most cases there was no rise in pressure at this position - to correspond to the rise resulting from the fast burning downstream of the obstacle - until some time after the pressure measured by the transducers closer to the obstacle reached a maximum value and began to decay. Since no pressure gradient was measured between the test vessel exit and the dump vessel during this phase, then no gas venting was taking place. While there was no gas movement at the plane of the tube exit, the unburnt gas at a few tube-diameters upstream was being compressed up to pressures of over 3 bara by a flame travelling with speeds of up to 600 m/s. This would indicate a strong blast wave propagation with an associated pressure determined by the inertia of the gas ahead of it that was not influenced by the presence of the vent.

Figure 2 compares the flame speeds predicted by Eq. 1, using the pressure record of the single-bar test (in Fig. 1) with the experimental measurements. For the first 60 ms of the test, during which time the flame was upstream of the obstacle, higher flame speeds than those measured would be needed to predict the overpressure on the basis of the mechanism of Eq. 1. The explosion development in this section of the vessel is effectively a relatively slow explosion, venting unburnt gas through the restriction provided by the obstacle. The mechanism of pressure generation is therefore quite different from that implied by Eq. 1. On the other hand, the good agreement obtained downstream of the obstacle supports the premise that the pressure generation in this region was due to the inertia of the gas ahead the fast accelerating high speed flame. Strehlow et al [10] showed that a constant speed flame and an accelerating flame with the same maximum flame speed would generate equivalent blast waves.

Figure 3 shows a plot of recorded maximum overpressure (for all repeat tests) against the characteristic obstacle-scale. The scale of the obstacle was varied by changing either the blockage ratio (for a fixed number of bars) or the number of bars (for a fixed blockage ratio). The data is grouped for constant blockage ratio and for each set the overpressure increased as the obstacle-scale increased. For the same obstacle-scale the overpressure was generally higher for higher blockage ratios. However, the relative increase in overpressure with increasing blockage ratio decreased as

the blockage ratio increased. The overpressures at blockage ratios of 55, 60 and 70 % are shown to effectively be on the same line. At these blockages the overpressure was apparently independent of the blockage ratio and dependent only on scale. Furthermore, the large scale (single-bar, 111 mm) 80% BR tests gave lower overpressures than those given by the lower scale single-bar obstacles at BRs of 70 and 60 and 55 %. As will be quantified below, increasing blockage ratio increases the rms turbulent velocity u' and hence the overpressure increases as the mass burning rate increases. The levelling off of the overpressures (for the same obstacle-scale) for $BR > 55\%$ and the observed reduction at $BR = 80\%$ would indicate the onset of a counter-acting mechanism, such as turbulent flame quenching.

Estimation of turbulent combustion parameters

Phylaktou and Andrews [11] presented a method to predict the maximum turbulence levels generated downstream of a grid plate obstacle by an explosion induced flow. For thin sharp obstacles they showed that the turbulence intensity is given by,

$$u'/U = 0.225\sqrt{K} \quad (2)$$

where K is the pressure loss coefficient and U is the mean velocity of the flow induced ahead of the flame, determined from transient differential pressure measurements across the obstacle [7].

Measurements of the length-scale of turbulence ℓ , immediately on the downstream side of grid plates have been carried out by Baines and Peterson [12] and Checkel [13]. This data was analysed and it was found that at the position of maximum turbulence, ℓ ranged from 30 to 80 % of the characteristic grid-scale, b [14]. Recent experimental measurements of ℓ by Shell Research Ltd. [15] showed that $\ell = b$ at the plane of maximum turbulence and this was the largest length scale measured in the flow. In view of the uncertainties of the previous measurements it was decided to adopt $\ell = b$ for the evaluation of the integral length-scale of turbulence in the present work.

Evaluation of u' and ℓ enabled the calculation of the turbulent Reynolds number R_t and the Karlovitz number Ka in the region of maximum flow turbulence downstream of the obstacle just prior to flame arrival, according to Eqs. 3 and 4 [16]

$$R_t = u' \ell / \nu \quad (3)$$

$$Ka = 0.157(u'/S_L)^2 R_t^{-0.5} \quad (4)$$

The Karlovitz stretch factor is a measure of the flame straining. At sufficiently high turbulence levels (and thus high straining) the flame front becomes fragmented and is partially or totally quenched. This number is fundamentally defined as the ratio of chemical to turbulent lifetimes [17]. The turbulent lifetime decreases with increasing turbulence levels and thus Ka increases. In theory, flame quenching occurs when $Ka > 1$, but the actual threshold value may be different, depending on the definition and approximations employed in the quantification of Ka [16,18].

The measured explosion-induced mean gas flow velocities (U) ahead of the flame just prior to its interaction with the obstacle are shown in Table 1, along with the other calculated turbulent combustion parameters for each test condition. Corrections for isentropic compression at the time of flame arrival at the obstacle resulted in minor variation of the mixture kinematic viscosity and laminar burning velocity. The latter was taken to be 0.45 m/s at standard temperature and pressure [19]. The turbulent Reynolds number ranged from 4,000 to 215,000 and this covers the range encountered in practical turbulent combustion systems and large scale vapour cloud explosions. In terms of the Borghi flame-structure phase diagram [20], defined by the parameters u'/S_L and ℓ/δ_L ,

the majority of the present tests lie well within the “thickened-wrinkled flame with possible extinctions” regime or in terms of the terminology of Peters [21], in the “distributed reaction zone”.

The influence of Karlovitz stretch factor

As shown in Table 1, for a number of tests the Karlovitz number was greater than 1, which is the theoretical limit above which flame extinction is predicted (see earlier discussion). It should be noted that total flame extinction was not observed in any of the present tests. In all cases the explosion propagated strongly, generating significant overpressures. However, some definite influence of the Karlovitz number was observed and is presented below.

Figure 4 plots the maximum pressure against Ka for a series of tests with approximately constant obstacle scale, as shown. The increase in Ka was achieved by increasing the maximum u' (see Eq. 4) from about 3 to 25 m/s by increasing the blockage ratio and the scale was kept constant by simultaneously increasing the number of bars. Up to approximately $Ka = 1$ there was an increase in maximum pressure with increasing u' and this may be attributed to the effect of u' rather than to the Karlovitz number directly. However, any further increases in u' which in effect increased Ka to values greater than unity, resulted in slightly reduced, but fairly constant pressures independent of Ka . It is worth noting at this point that in the present system the turbulence was non-uniform, highly anisotropic in the immediate region downstream of the obstacle and decaying further downstream. It would appear that for these high Ka number tests, the flame did not burn in the regions of maximum turbulence until levels of u' had decayed to a lower effective value, ca 13 m/s, (and thus lower local Ka) which would have allowed flame propagation.

For the tests in Fig. 5 both the scale and the turbulence levels were increased simultaneously. The maximum pressure increased strongly to over 2.5 bar, until Ka exceeded unity, at which point a reduction of pressure was observed despite the further increase in both scale and turbulence. In this plot it would appear that the critical Ka was lower than 1, however this might be simply due to the lack of data points for Ka near unity. This plot demonstrates that at larger scales it is possible to induce higher levels of turbulence without entering the flame quenching regime and thus result in significant overpressures which are not possible at smaller scales (cf. Fig. 4), unless the Karlovitz number is maintained below 1, through perhaps an increase in the value of the laminar burning velocity S_L (see Eq. 4). This in fact is the technique used by British Gas [2] and Shell Research [1] in the development of their explosion scaling methodologies, although in the Shell work the increase in reactivity was intended to maintain the compressibility effects at small scale rather than to influence Ka .

Both Figs. 4 and 5 suggest that the Ka number may be acting as a switch between full - burning and partial-burning at a critical value of around unity rather than having a continuous influence over the range of values.

The influence of scale and Reynolds Number

From all the tests in this study, those carried out with the 30% BR and different number of bars (see Fig. 3) effectively isolate the effect of obstacle-scale (or turbulent integral length-scale) on the overpressure. The Karlovitz number was low and approximately constant (0.15 – 0.30) and the rms turbulent velocity was also fairly low and constant (4.4 - 4.7 m/s). The plot of these tests in Fig. 3 suggests a fairly strong dependence of pressure on scale.

In all the tests only u' and ℓ were intentionally changed. The appropriate dimensionless number that might incorporate their combined influence is the turbulent Reynolds number, R_t (Eq. 3). Figure 6 (continuous line curves - LHS axis) is a plot of the measured maximum pressure against R_t . The data separated into two distinct groups identified by their Karlovitz number range. This is effectively a reiteration of the previous observation that at the critical value of $Ka = 1$ there

was a sharp transition to partially quenched combustion with consequent lower overpressures, for the same R_f values.

The equations of the fitted lines for the two combustion regimes are as follows

$$P_{\max} = 0.017R_f^{0.43} \text{ (baro)} \quad \text{for } Ka \leq 1.0 \quad (5)$$

$$P_{\max} = 0.044R_f^{0.31} \text{ (baro)} \quad \text{for } Ka > 1.0 \quad (6)$$

The single point between the two lines corresponds to a test with $Ka=1.00$ and it would suggest that it defines the critical transition Ka . Furthermore, the point at the highest R_f corresponds to a $Ka=1.05$ and this would suggest a very sharp transition boundary between the two regimes. On the other hand, the limited number of data points on this plot means that the above deductions are speculative and it is possible that more points on this plot may reveal a more systematic influence of Ka .

The rate of pressure rise is an important parameter in turbulent explosions as it is related to the mass burning rate, and it is also critical in structural response design. The maximum rate of pressure rise (as indicated in Fig. 1) was measured (by differentiating the smoothed pressure signal) and found to correlate well with maximum pressure according to

$$P_{\max} = 0.037 \left(\frac{dP}{dt} \right)_{\max}^{0.54} \text{ (bar/s)} \quad (7)$$

Graphical correlation of $(dP/dt)_{\max}$ against R_f produced the following equations in agreement with derivation of dependence through manipulation of Eqs. 7, 6 and 5.

$$\left(\frac{dP}{dt} \right)_{\max} = 0.248R_f^{0.788} \text{ (bar/s)} \quad \text{for } Ka \leq 1.0 \quad (8)$$

$$\left(\frac{dP}{dt} \right)_{\max} = 2.45R_f^{0.514} \text{ (bar/s)} \quad \text{for } Ka > 1.0 \quad (9)$$

A TURBULENT BURNING VELOCITY CORRELATION

The applicability of Eq 1 to the present experiments was validated earlier and it was used to obtain the maximum flame speeds corresponding to the measured maximum overpressures. On the assumption that the flame speed is also given by the product of the adiabatic expansion factor and the turbulent burning velocity, $S_f = E S_T$, it was possible to obtain S_T (E was assumed constant at 7.5, ignoring any compressibility, flame-thickness and heat loss effects).

Figure 6 (dashed-line curves - RHS axis) shows the derived S_T as a function of R_f , for the two Ka ranges. The correlating equations were

$$S_T = 3.01R_f^{0.27} \text{ (m / s)} \quad \text{for } Ka \leq 1 \quad (10)$$

$$S_T = 5.15R_f^{0.20} \text{ (m / s)} \quad \text{for } Ka > 1 \quad (11)$$

It should be noted that in the present tests the kinematic viscosity of the mixture was not a variable. The implicit dependence on this parameter, indicated in Eqs. 10 and 11 (and in previous equations), was therefore not validated. However, the other two parameters defining R_f (ℓ and u') were the main variables in this study. Additionally their individual influence on S_T was verified by multi-variant regression analysis for the $Ka \leq 1$ regime (where more data points were available) as

$$S_T = 67.9u^{0.25 \pm 0.03} \ell^{0.29 \pm 0.02} \quad (\text{m/s}) \quad \text{for } Ka \leq 1 \quad (12)$$

therefore the dependence on R_ℓ indicated in Eq. 10 is an acceptable compromise of the individual dependencies.

By substituting for R_ℓ using Ka (Eq. 4), Eq. 10 can be rewritten as

$$S_T \propto \frac{u'^{1.08}}{Ka^{0.54}} \quad (13)$$

Bradley et al [22] proposed the power law (for $Le=1$ and $Ka = 0.01$ to 0.63)

$$S_T \propto \frac{u'}{Ka^{0.3}} \quad (14)$$

In general terms these expressions are similar, however in terms of actual dependencies it can be shown that Eq. 14 gives $S_T \propto u'^{0.55} \ell^{0.15}$ compared to the exponent of 0.27 for both variables in the present correlation.

For combustion in the distributed reaction zone Gulder [23] proposed

$$S_T \propto u'^{0.25} S_L^{0.75} \quad (15)$$

which shows good agreement with Eq. 12 with regard to the dependence on u' but it shows no influence of scale.

Again, for the distributed reaction combustion regime Damkohler [24] proposed

$$S_T \propto u' Da^{0.5} \propto \frac{u'}{Ka^{0.5}} \quad (16)$$

which is in close agreement with the present correlation - Eq. 13.

Based on fractal theory, Gouldin [25] proposed

$$S_T/S_L \propto R_\ell^{0.26} \quad (17)$$

which is in good agreement with Eq. 10. However, the fractal concept of this model applies to a continuous uniformly-disturbed surface and therefore it could be argued that this concept is not valid in the distributed reaction zone. Nevertheless, Shell Research [1] have employed this model in developing their explosion scaling methodology. The relative success [26] of this approach would indicate that the scale dependence predicted by Eqs 17 and 10 might be correct.

CONCLUDING REMARKS

In this study the turbulent Reynolds number of methane/air explosions was systematically changed by varying both the scale and intensity of turbulence. The maximum overpressure, rate of pressure rise and flame speed increased with an increase of R_ℓ . This trend was also influenced by the Karlovitz number. There was evidence that Ka may be acting as a switch between full -burning and partial-burning at a critical value of around unity rather than having a continuous influence over the range of values.

It was shown that at larger scales it is possible to induce higher levels of turbulence without entering the flame quenching regime. Significant overpressures would result which are not possible at smaller scales, unless the Karlovitz number is maintained below 1, through perhaps an increase in the laminar burning velocity of the mixture.

The overpressures and the estimated burning velocity S_T were shown to correlate well with R_t in the range of 4000 to 215000. The data was shown to separate into two distinct correlations identified by $Ka \leq 1$ and $Ka > 1$. This indicated that at the critical value of $Ka = 1$ there was a sharp transition to partially quenched combustion with consequently lower overpressures, for the same R_t values. There was no evidence of total flame quenching in any of the tests.

This indicates that caution should be used when applying isotropic-turbulence flame-quenching criteria in turbulent explosion modelling. In explosions the turbulence generated by obstructions is highly anisotropic (and transient) and it may be ignited by strong ignition sources (such as jetted flames rather than small sparks). In regions of high turbulence the flame may quench locally, but parts of the flame front could propagate through regions of lower turbulence and therefore the explosion would be sustained and could still result in significant overpressures. Even in the case of complete turbulent flame extinction, the decaying nature of turbulence may allow re-ignition of the mixture by the hot combustion products.

The dominant combustion regime in the present tests was identified as that of a distributed reaction or a fragmented flame front. The S_T correlation (at low Ka) compared well with turbulent combustion models that specifically refer to combustion in the distributed reaction zone.

Figure 6 (and the associated correlations) may provide a basis for predicting maximum explosion overpressures and also for designing scaled explosion experiments for more detailed investigation of the explosion development. They appear to bring together a number of features that have been found to be partially successful in explosion scaling practice to date.

NOMENCLATURE

| | |
|----------|---|
| α | speed of sound |
| ρ | density of the fluid |
| γ | specific heat ratio |
| ν | viscosity of the mixture |
| (dP/dt) | rate of pressure rise |
| b | characteristic obstacle-scale / bar width |
| BR | blockage ratio |
| D | diameter of tube |
| Da | Damkohler number (=1/Ka) |
| E | expansion ratio |
| K | pressure loss coefficient |
| Ka | Karlovitz number |
| ℓ | integral length-scale of turbulence (= b) |
| L | length |
| Le | Lewis number |
| M | Mach number |
| P | pressure or overpressure |
| R_t | turbulent Reynolds number |
| S_f | flame speed |
| S_L | laminar burning velocity |
| S_T | turbulent burning velocity |
| U | mean velocity of the flow |
| u' | root mean square (rms) turbulent velocity |

ACKNOWLEDGEMENTS

We thank the Engineering and Physical Sciences Research Council and the Health and Safety Offshore Division for supporting this work.

REFERENCES

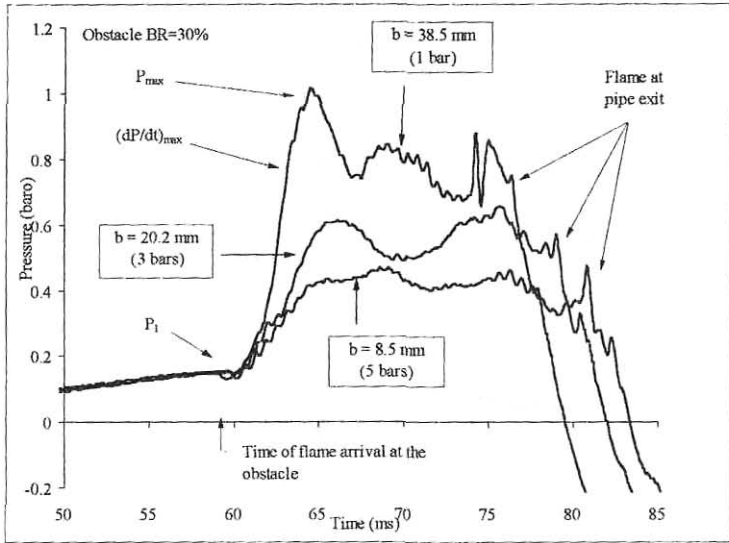
1. Taylor, P.H. and Hirst, W.J.S., *Twenty-Second Symposium (International) on Combustion*, The Combustion Institute, 1989.
2. Catlin, C.A. and Johnson, D.M., *Combust. Flame* 88:15 (1992).
3. Phylaktou, H. and Andrews, G.E., *Trans IChemE*, 73, Part B (1995).
4. Harrison, A.J. Eyre, J.A., *Societe de Chemie Industrielle*, Paris, 1986, 1, p.38.
5. Harrison, A.J. Eyre, J.A., *Combust.Sci.Technol.*, 52:121 (1987).
6. Abdel-Gayed, R.G. and Bradley, D., in *Fuel Air Explosions*. (J. Lee, C.M. Guirao and D.E. Grierson, Eds.), University of Waterloo Press, Montreal, 1982, p.51.
7. Phylaktou, H. and Andrews, G.E., *Combust. and Flame*, 85: 363 (1991).
8. Harris, R.J. & Wickens, M.J., *The Institution of Gas Engineers*, 55th Autumn Meeting, Communication 1408, 1989.
9. Taylor, G. I., *Proc. Roy. Soc. London*. Series A, 186:273-292 (1946)
10. Strehlow, R.A., Luckritz, R.T., Adamczyk, A.A. and Shimpf, S.A., *Combust. And Flame* 35:297-310 (1979)
11. Phylaktou, H. and Andrews, G.E., *25nd Symposium (International) on Combustion*, The Combustion Institute, 1994, p 103
12. Baines, W.D. and Peterson, E.G., *Trans. ASME* 73:167.(1951)
13. Checkel, M.D., 1981, Turbulence Enhanced Combustion of Lean Mixtures, Ph.D Thesis, Cambridge University.
14. Phylaktou, H., 1993, Gas Explosions in Long Closed Vessels with Obstacles, PhD Thesis, University of Leeds
15. Mercx, W.P.M. (project Co-ordinator), Modelling and Experimental Research into Gas Explosions, Overall final report, CEC contract: STEP-CT-0111 (SSMA), 1995.
16. Abdel-Gayed, R.G., Al-Kishali, K.J. & Bradley, D., *Proc. R. Soc. Lond.*, A 391, p.393. (1984)
17. Karlovitz, B., *Selected Combustion Problems* Butterworths, London, 1954, p248.
18. Chung, S.H., Chung, D.H., Fu, C. and Cho, P., *Combust. Flame* 106: 515-520 (1996)
19. Andrews, G.E. and Bradley, D., *Combust. Flame*, 19, p.275 (1972)
20. Borghi, R., *Recent Advances in Aerospace Science* (Bruno, C. & Casci, C. Ed.), Plenum, 1985, p.117.
21. Peters, N., *Twenty-first Symposium (International) on Combustion*, The Combustion Institute, 1988, p 1231
22. Bradley, D., Lau, A.K.C. and Lawes, M., *Phil. Trans. R. Soc Lond.*, A 338:359 (1992)
23. Gulder, O.L., *Twenty third Symposium (International) on Combustion*, The Combustion Institute, 1990, p.743.
24. Damkohler, G., Z., *Elektrochem.* 46: 601(1940) (English translation NACA TM 112, 1947)
25. Gouldin, P. C., *Combust. Flame*, 68: 249-266 (1987)
26. Mercx, W.P.M., Johnson, D.M. and Puttock, J., *Process Safety Progress* 14 No2:120-130 (1995)

| Test No | BR % | Number of bars | b= ℓ mm | U m/s | u'/S _L ^a | R _t | Ka | ℓ/δ_L ^b |
|---------|------|----------------|--------------|-------|--------------------------------|----------------|------|------------------------------|
| 1 | 20 | 1 | 25.6 | 23.9 | 6.0 | 4787 | 0.08 | 793 |
| 2 | 30 | 1 | 38.5 | 23.7 | 10.3 | 12299 | 0.15 | 1198 |
| 3 | 30 | 2 | 20.2 | 23.1 | 10.0 | 6308 | 0.20 | 631 |
| 4 | 30 | 3 | 13.7 | 22.5 | 9.7 | 4163 | 0.23 | 428 |
| 6 | 30 | 5 | 8.5 | 23.0 | 9.9 | 2634 | 0.30 | 265 |
| 5 | 40 | 1 | 51.8 | 24.1 | 16.0 | 25807 | 0.25 | 1613 |
| 7 | 40 | 2 | 27.0 | 23.6 | 15.7 | 13163 | 0.34 | 838 |
| 8 | 55 | 1 | 70.0 | 21.8 | 25.4 | 56701 | 0.42 | 2235 |
| 9 | 60 | 1 | 79.7 | 20.0 | 28.5 | 72766 | 0.47 | 2549 |
| 11 | 60 | 3 | 28.3 | 20.7 | 29.5 | 26573 | 0.84 | 900 |
| 10 | 70 | 1 | 94.8 | 18.7 | 39.8 | 125450 | 0.70 | 3148 |
| 12 | 70 | 2 | 49.3 | 18.9 | 40.4 | 65836 | 1.00 | 1631 |
| 14 | 70 | 3 | 33.5 | 18.7 | 39.9 | 44261 | 1.19 | 1109 |
| 15 | 70 | 5 | 20.6 | 18.3 | 39.2 | 26341 | 1.48 | 673 |
| 13 | 80 | 1 | 111.3 | 15.9 | 55.8 | 214319 | 1.05 | 3843 |
| 16 | 80 | 4 | 29.6 | 15.4 | 54.2 | 54409 | 1.98 | 1003 |

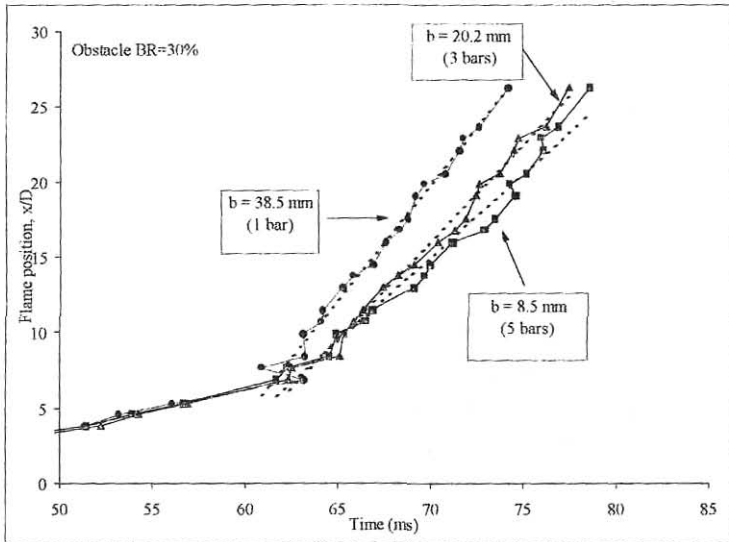
Table 1. Test conditions, measured and calculated combustion parameters.

^a The laminar burning velocity was constant (10% CH₄/air (v/v) S_L=0.45)

^b laminar flame thickness, $\delta_L = v/S_L$. This gives a thickness that is about 1/30th of the actual experimentally determined value of 1 mm. Nevertheless this approximation is implicit in the evaluation of Ka and a number of turbulent combustion regime diagrams are defined in terms of this approximation.



(a)



(b)

Fig. 1 (a) Pressure-time histories and (b) corresponding flame position against time for tests with obstacles of different scales at constant BR = 30%.

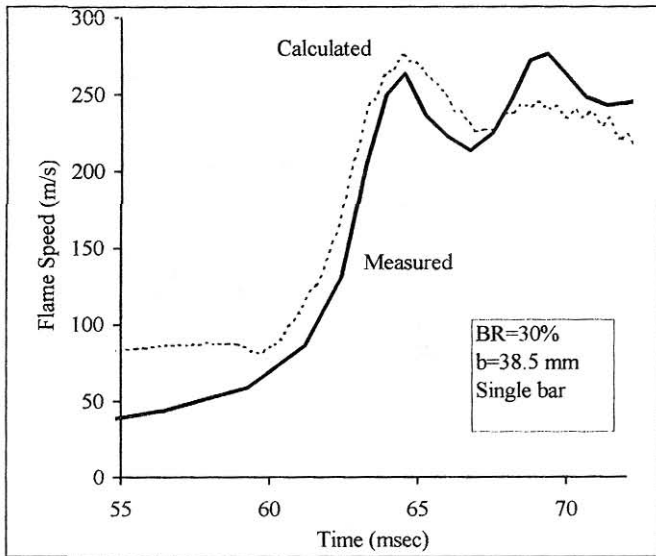


Fig. 2. Measured flame speed history compared to that calculated using Eq. 1 for the single-bar, 30% BR test.

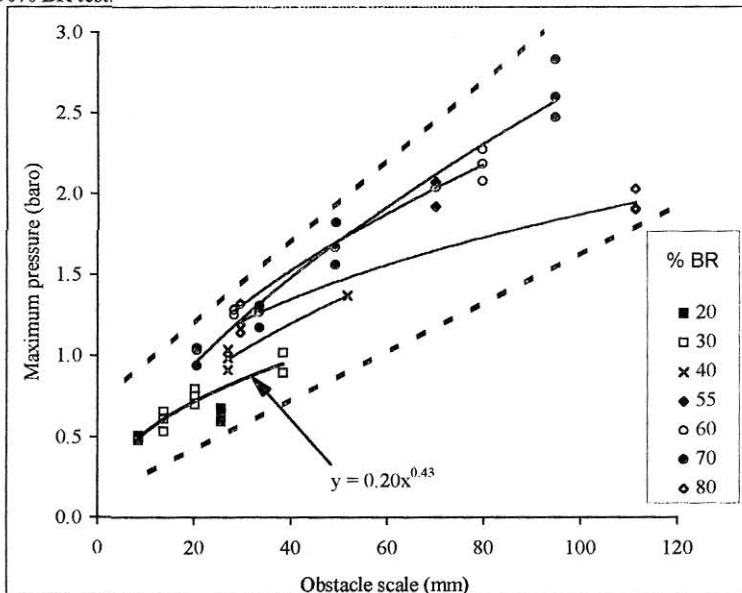


Fig. 3. Variation of maximum overpressure with scale for all blockage ratios tested. (Equation shown is for the line fitted to 30% BR data. See text)

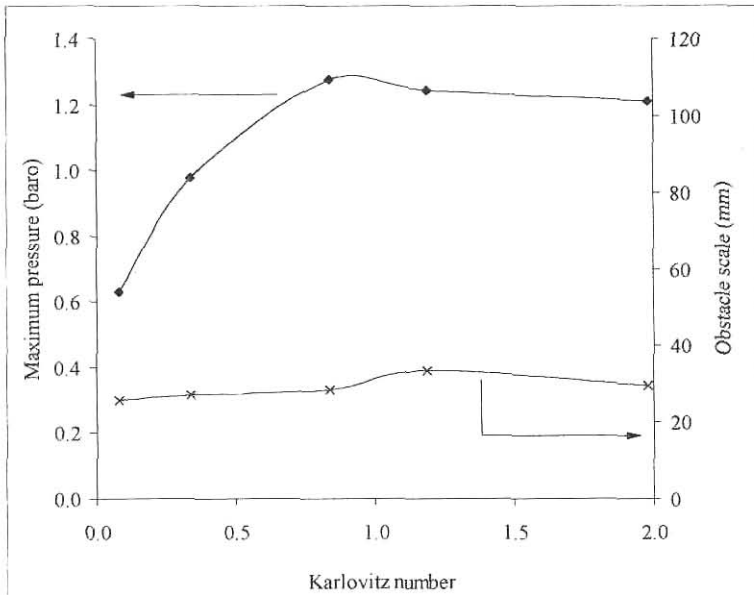


Fig. 4. Variation of maximum overpressure with Ka for approximately constant obstacle-scale (increasing u').

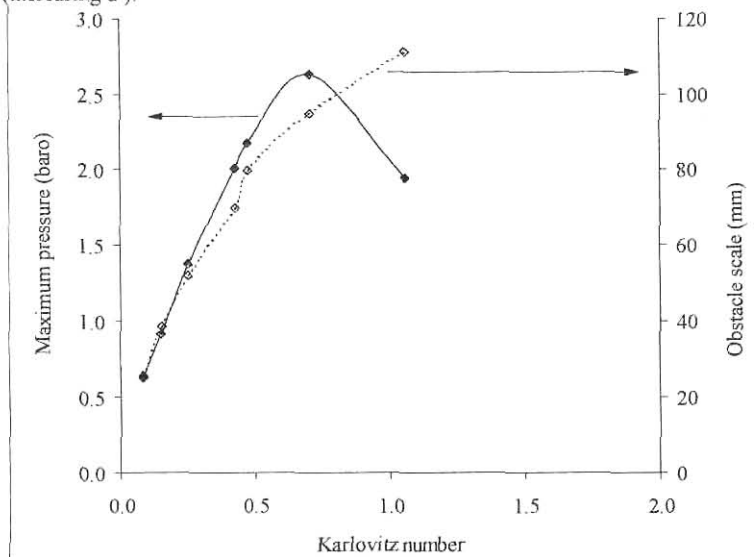


Fig. 5. Variation of maximum overpressure with Ka for obstacles of increasing scale. This illustrates the combined effect of u' and scale.

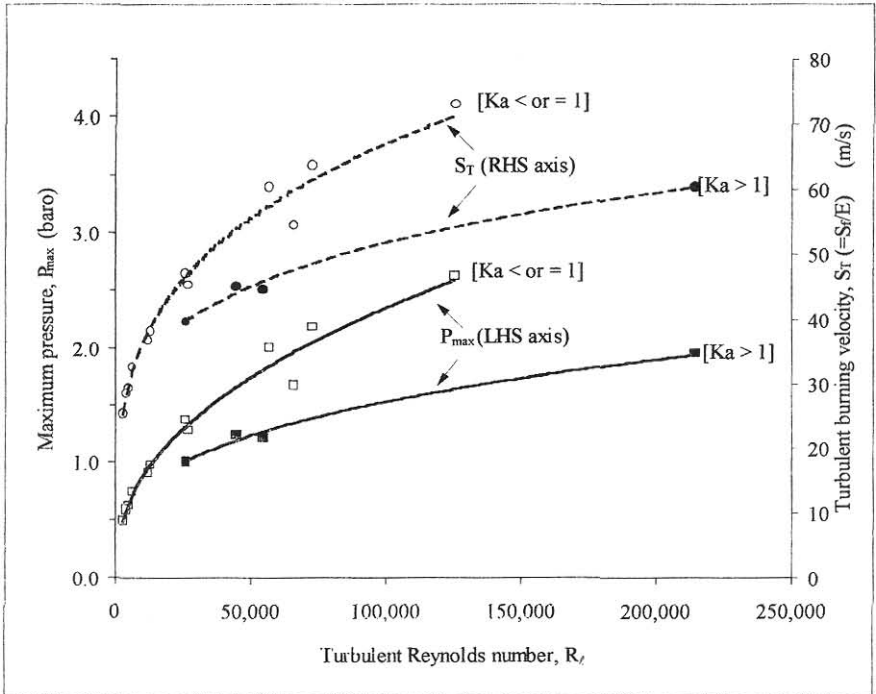


Fig. 6. Maximum overpressure (LHS axis) and turbulent burning velocity (RHS axis) plotted against R_t for the data sets, $[Ka > 1]$ and $[Ka \leq 1]$.